Preliminary broadband modelling of an Alpine fault earthquake in Christchurch

C. Holden J. Zhao

GNS Science Report 2011/28
July 2011

GNS SCIENCE
TE PŪ AO

DISCLAIMER

The report includes preliminary ground motion estimates for a potential Alpine Fault earthquake. These estimates have been computed in a deterministic way, based on our current knowledge of fault mechanics, and applying a validated methodology for large crustal earthquakes using conservative parameters. Although all reasonable effort is made in arriving at the estimates there is uncertainty inherent within the nature of natural events. For this reason, GNS Science cannot accept responsibility for any actions taken based on the estimates and excludes liability for any loss, damage or expense in any way resulting from those actions.

EMBARGO

This report needs to be embargoed until the Royal Commission's Report is completed, currently scheduled for mid-October.

Thus, please ensure the reports are not disseminated until GNS Science gives clearance to do so. GNS Science will, however, need to provide copies for the Royal Commission, but final electronic versions will be fine for this purpose.

BIBLIOGRAPHIC REFERENCE

Holden, C. and Zhao, J. 2011. Preliminary broadband modelling of an Alpine fault earthquake in Christchurch, *GNS Science Report* 2011/28. 19 p.

C. Holden, GNS Science, PO Box 30368, Lower Hutt
J. Zhao, GNS Science, PO Box 30368, Lower Hutt

978-0-478-19852-2

ISSN 1177-2425
ISBN 978-0-478-19852-2

CONTENTS

FIGURES

TABLES

ABSTRACT

We have computed broadband synthetic seismograms in Christchurch for a large possible Alpine fault earthquake. In this preliminary study, we chose conservative values for all source parameters based on our current understanding of large crustal earthquake source mechanics. By using conservative parameters, we are attempting to model maximum possible ground shaking intensity. We computed the ground motion for generic rock sites in Christchurch. We subsequently superimposed the effects of soft soil condition on the modelled ground motions.

Calculations for synthetic seismograms are based on a validated algorithm for large crustal earthquakes. Large accelerations are generated from localized asperities while the ground motions resulting from the rest of the fault rupture area are negligible. We distributed asperities where large surface fault displacements have been inferred from paleoseismic studies. For each asperity, records from a small or moderate earthquake were used as proxies for the Green's functions. As such, they account for path effects incurred during propagation of the waves from the earthquake to the receiver site. Site effects for soft ground conditions were also added to account for possible amplification of ground shaking by soil layers in Christchurch.

The preliminary estimates for peak horizontal acceleration are less than 4% g. These results are reasonably consistent with recorded values from recent large earthquakes (Mw > 7) and distances of 150 km+.

KEYWORDS

Alpine Fault; Modelling; Christchurch.

1.0 INTRODUCTION

The Alpine Fault is a major geological feature in New Zealand. It is a dextral transform fault separating the Pacific plate on the east from the Australian plate on the west, crossing the South Island from Northeast to Southwest (Figure 1). It has an average slip rate of 40 mm per year and is the longest fault in New Zealand with a length, on land, of 650 km (Yetton, 2000).

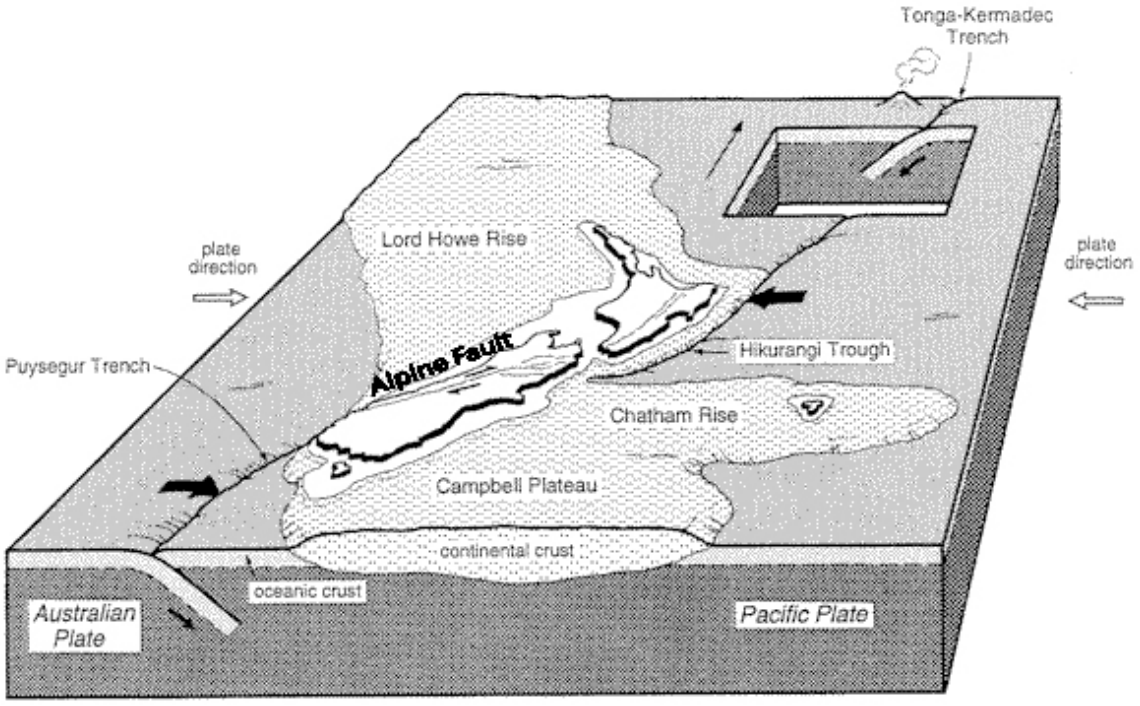

Figure 1 New Zealand regional tectonics (from Ansell and Taber, 1996). Heavy black arrows indicate subduction.

The Alpine Fault is a potential source of major earthquakes in the near future. The return period of the fault is approximately 270 years, with no major event occurring over the last 294 years. Sutherland et al. (2007) suggested that a magnitude Mw> 8 would be a realistic scenario for a future Alpine fault rupture.

The large September 2010 and the tragic February 2011 Canterbury earthquakes caused widespread damage by ground shaking and sand liquefaction in the Christchurch region. Both earthquakes are at a short distance from the Christchurch central business area and have a magnitude that is much smaller than the expected one of the Alpine fault (Mw=8.2). The Alpine fault is at a distance of 130km (the closest distance to the fault) from Christchurch and there is a need to better assess the effect of ground shaking in Christchurch from this large event. We will model broadband ground-motion in Christchurch from a magnitude 8.2 Alpine Fault event. The results are preliminary and further studies will be required to provide detailed analyses and assess the effect of fault parameters used in the present preliminary study.

The technique is based on the recipe for modelling large crustal events developed by Irikura and Miyake (2011). The seismograms were calculated using an empirical Green's function approach, where the empirical Green's functions – the ground-motions from discretized parts

of the fault are summed according to the formulation of Irikura (1986) and Kamae and Irikura (1998), and local site effects are modelled by using an equivalent linear site modelling approach.

In order to consider an extreme shaking scenario, all the results in this study represent the most conservative level of ground shaking in Christchurch within the range of possible fault parameters adopted in the present study.

2.0 METHODOLOGY

2.1 The recipe

We based our study on Irikura and Miyake (2011) assumption that large accelerations are generated from asperities while the ground motions from the rest of the fault rupture area are negligible. They propose a recipe based on a characterized source model for large earthquakes following three parameters: outer parameters describing the source size and magnitude, inner parameters describing heterogeneities on the fault (asperity size and stress drop) and extra parameters describing the rupture initiation and velocity.

2.2 The empirical Green's function method

Ground motion at a particular site is characterized by a source effect, a propagation path effect and a site effect. An efficient way to model the effect of propagation path is to use recordings of a small earthquake or empirical Green's functions that contain the effect of propagation for the large event we attempt to model. The Green's function is from an event with a sufficiently small magnitude compared to the large event. The ground motions generated by the small events are then scaled and summed to compute the ground motions from the large event according to the formulation developed by Irikura (1986) and Kamae and Irikura (1998).

The alpine fault is 500 km long and the propagation path effects from each of the asperities at different locations along the fault to Christchurch vary strongly. To model this effect we will use a small earthquake records for each of the modelled asperities, rather than using one record to account for the averaged path effect for the whole fault length.

2.3 Site effects

It is not possible to select small earthquake records that were recorded at a site with similar site conditions for different parts of Christchurch as the Green's functions. In the present study, the empirical Green's functions are the small earthquake records from rock sites and the site effect will then be modelled using 1-D equivalent linear model for a representative site in Christchurch and the synthetic ground motions as the excitation.

3.0 SOURCE DESCRIPTION

The Alpine Fault is a striking feature in the South Island and runs for 800 km offshore and onshore. It has ruptured in recent large earthquakes with magnitudes estimated at 7.9±0.3, 7.6±0.3 and 7.9±0.4 (Sutherland et al., 2007). The fault strike at 52 degrees, dips at 45 degrees and is a pure right-lateral strike-slip. Recent studies by Sutherland et al. (2007)

suggested a likely future event to have a magnitude of 8.2, with a rupture length of 500 km long, including a 100km long offshore segment. The seismogenic width from their study is approximated to 12 km. The section in the central part of the South Island, between Haast and WVZ (Waitaha Valley) has characteristics of stable sliding conditions such as high fluid pressures and geothermal gradient (Sutherland et al. 2007) with little coseismic slip in previous events (Figure 2). Past large events have generated offsets of a few metres at the north of WVZ (Figure 2), and up to 9 m on the offshore segment, around Milford sound (MSZ) and nearby JCZ. In the following sections these segments with a large slip are assumed to be the major asperities (represented as yellow ellipses on Figure 2).

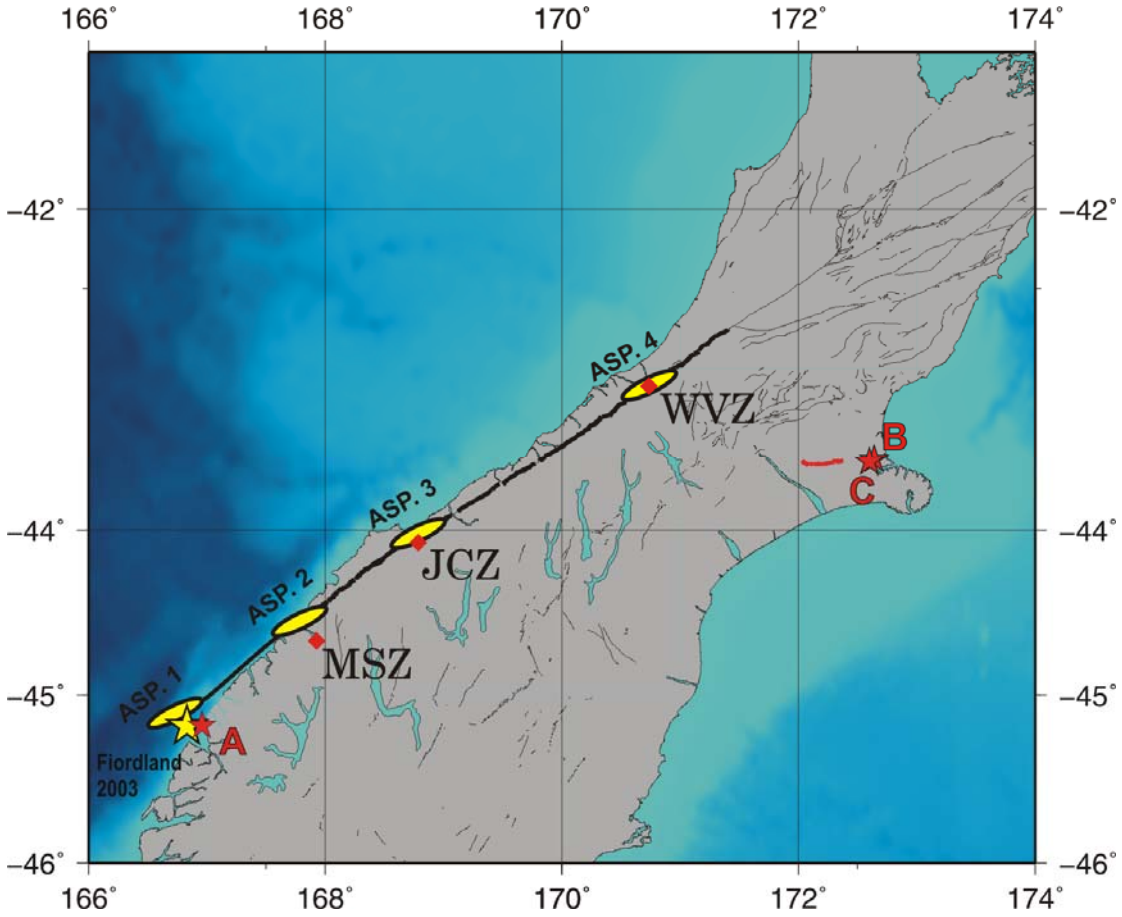

Figure 2 Map of the South Island and active faults. The bold line is the length of the likely Alpine fault rupture; the red line is the fault trace from the Mw 7.1 Darfield earthquake; the yellow ellipses represent the major potential asperity locations and the sizes of the asperities on the Alpine fault; the red stars are the hypocentral locations for 2 Canterbury aftershocks and an aftershock of the Mw 7.2 Fiordland earthquake. The records from these aftershocks are used as empirical Green's functions. The red diamonds are the locations of strong motion stations.

4.0 BROADBAND MODELLING FOR A ROCK SITE CONDITION

4.1 Characterized Alpine fault source model

Following Irikura and Miyake (2011) recipe on modelling strong ground motion for large earthquakes, we inferred the following characterized source model for an Alpine fault earthquake. Mw 8.2 is over the magnitude range of the recipe, we set the rupture area between the estimates between Somerville et al. (1999) and Irikura and Miyake (2011).

4.1.1 Outer parameters

- Magnitude Mw 8.2
- Total rupture area 6000 (500 by 12) km^2
- Total Seismic Moment: 2.24x1021Nm

4.1.2 Inner parameters

We used the empirical scaling relation from Somerville et al. (1999) relating asperity area to total rupture area and the estimated asperity area is 1300 km^2 (around 22%). The 3 largest asperities as described in the source paragraph give an average (and rounded) asperity area of 50 by 10 km^2. We artificially added a fourth asperity nearest to Christchurch in order to worsen the ground shaking.

We distributed the asperities at locations where very large coseismic ground displacements have been observed in previous events (Figure 2). The southern-most asperity (ASP1) is located about 100 km offshore, the second asperity (ASP2) is located onshore, near Milford Sound (MSZ), the third asperity (ASP3) is located near Jackson Bay (JCZ) and the fourth asperity (ASP4) is located at the northern part of the fault (WVZ), 170 km away from Christchurch . Descriptions of the asperities are summarized in Table 1.

Stress drop for each asperity is based on the value obtained from modelling the recent 2008 Mw 7.9 Wenchuan crustal event (Kurahashi and Irikura, 2010). They calculated a stress drop value of 13.6 MPa for asperities with similar rupture areas.

Table 1 Characteristics of the asperities

	Size (LxW)(km2)	Moment (Nm)	Mw	Stress drop (MPa)
Main Event	500x18	2.24×10^{21}	8.2	
ASP1	50x10	1.35×10^{20}	7.4	13.6
ASP2	50x10	1.35×10^{20}	7.4	13.6
ASP3	50x10	1.35×10^{20}	7.4	13.6
ASP4	50x10	1.35×10^{20}	7.4	13.6

4.1.3 Extra-parameters

Initiation of the rupture is likely to be south of the Alpine fault, where the fault is most strongly coupled. We are therefore modelling a South to North rupture.

4.1.4 Green's functions for asperity 1

We needed to have a strong-motion record from the asperity for the 100 km offshore segment of the Alpine fault. This location coincides with an Mw 7.2 earthquake in 2003 at 24 km depth. Conveniently this large earthquake provided us with many aftershocks that can be used as empirical Green's functions. However only one aftershock was recorded well-enough in Christchurch (MQZ). This aftershock, named "aftershock A" for our study had a magnitude Mw 6.0 and a focal mechanism similar to the modelled large event (Table 2).

4.1.5 Green's functions for asperities 2 to 4

At the time of this study there was no earthquake located near asperities 2 to 4 that had been recorded near Christchurch. However following the sequence of earthquakes in Christchurch since September 2010, there were many magnitude 5+ events recorded at sites near the asperities. The Green's function characterizing the ground between the source and receiver is the same for the receiver to the source. We decided to use aftershocks (B and C) of the Canterbury earthquakes as the Green's functions for our study.

We used aftershock B recorded at MSZ to characterize the path between Christchurch and the asperity 2, aftershock C recorded at JCZ to characterize the path between Christchurch and asperity 3, and aftershock C recorded at WVZ to characterize the path between Christchurch and asperity 4 (Table 2). To be consistent with the initial Alpine fault/Christchurch geometry we needed to reverse the North-South and East-West components).

Table 2 Characteristics of the Green's functions

	Green's function	Focal mechanism	Size (km^2)	Moment (Nm)	Mw	Stress drop (MPa)
ASP1	Aftershock A	52/38/84	10x10	$9.62x10^{17}$	6.0	1
ASP2	Aftershock B	246/84/169	2.6x2.6	$1.75x10^{16}$	4.8	1
ASP3	Aftershock C	60/65/154	2.5x2.5	$1.33x10^{16}$	4.7	1
ASP4	Aftershock C	60/65/154	2.5x2.5	$1.33x10^{16}$	4.7	1

4.1.6 Summing the asperities

The arrival time for each asperity to the receiver is the sum of the rupture time on the fault and the travel time from the source to the receiver. We assume a rupture velocity of 2.5 km/s. Travel times are based on an average velocity of 6 km/s. Rupture, travel and arrival times are summed up in Table 3.

Table 3 Distances and respective times for the asperities

	Distance to Christchurch (km)	Travel time (s)	Rupture time (s)	Dist. from hypocentre (km)	Arrival time (s)
ASP1	500	83	0	0	83
ASP2	400	66	40	100	106
ASP3	300	50	80	200	130
ASP4	170	28	160	400	188

4.1.7 Broadband seismograms

A set of horizontal broadband seismograms derived from a conservative scenario are shown in Figure 3. The portions of accelerograms with different colours represent the contribution from each asperity, with the purple one being the ground motion from asperity 4. The black accelerograms are the combined ground motion from each asperity with appropriate arrival time (Table 3). The maximum acceleration is less than 2% g, but the signal duration is quite significant as expected (over 300 sec). We also tested a lower stress drop value of 10 MPa for the asperities, as recommended by Dr Miyake (Pers. Com.). We adapted the parameters accordingly. As expected we obtained lower amplitude accelerograms (just over 100 mm/s/s for the maximum horizontal peak ground acceleration). Therefore for the purpose of this study, we kept the initial stress drop values of 13 MPa.

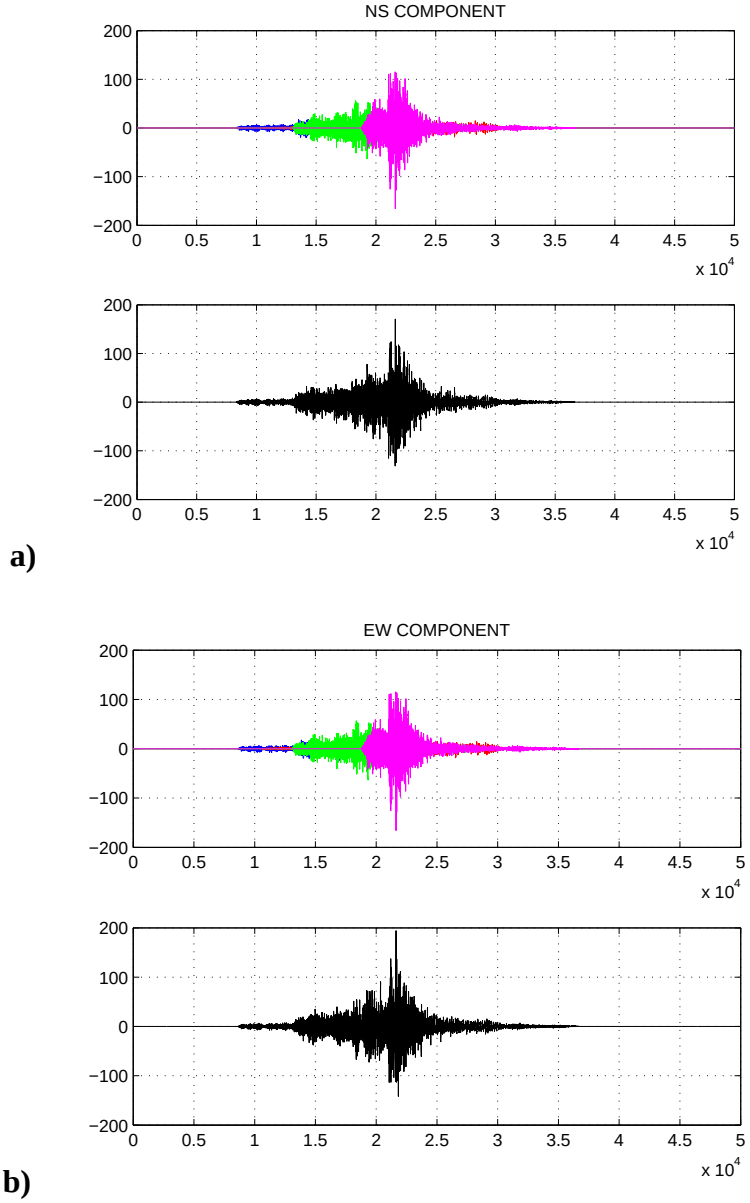

Figure 3 Broadband seismograms for North-South component (a) and east-West component (b) from individual asperity contribution (blue=asperity1, red=asperity 2, green=asperity 3, purple=asperity 4) and all asperities (black).

4.1.8 Spectral analysis

Figure 4 is showing the Fourier amplitude spectra for 3 selected small magnitude earthquakes (aftershocks B, C and D) recorded at stations MSZ, JCZ and WVZ, and for aftershock A recorded at MQZ (Christchurch). There are no other event with similar magnitude and location as aftershock A recorded at MQZ. The spectra are all consistent in their frequency amplitude distribution, apart from aftershock D at MSZ; however aftershock D was not used as an empirical Green's function in our study.

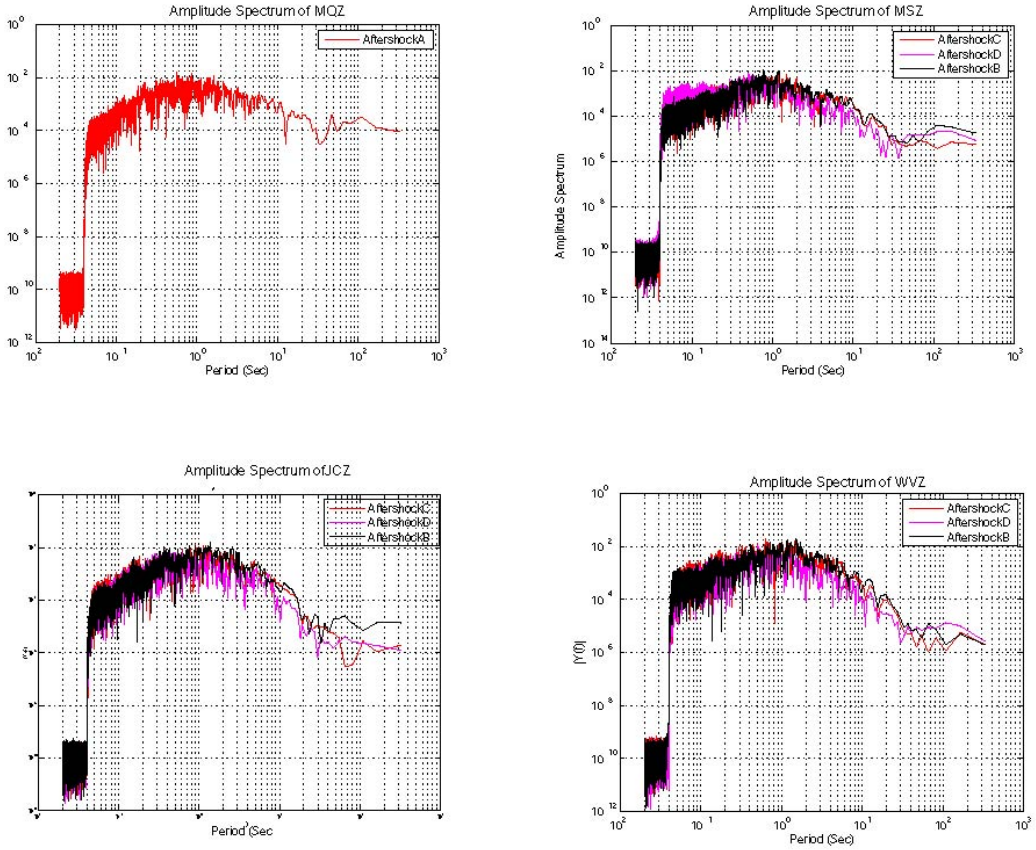

Figure 4 Amplitude spectra for 3 selected small magnitude earthquakes (aftershocks B, C and D) recorded at stations MSZ, JCZ and WVZ, and for aftershock A recorded at MQZ (Christchurch).

The Fourier spectra of the Green's functions do not show any particular peak amplitude, unlike the acceleration response spectra of the strong ground motion seismograms (**Figure 5**) which shows two dominant peaks at 0.18 second and 1.5 seconds. These peaks must be related to source effects since they do not show in the empirical Green's function spectra.

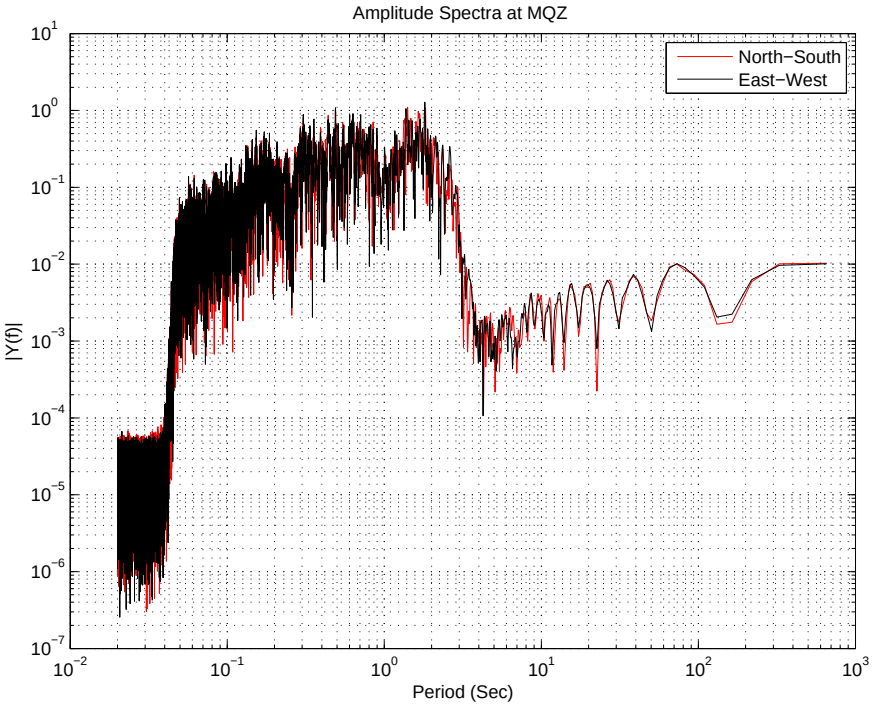

Figure 5 acceleration response spectra (5% damping) for the Alpine fault strong motion synthetic horizontal components.

5.0 SITE EFFECT MODELLED BY EQUIVALENT LINEAR MODEL FOR THE CHRISTCHURCH SITES

Most sites in the Christchurch Central Business District (CBD) are underlain by between 20 and 30 m of postglacial sediments comprising marginal marine sand and silt, and gravel-filled channels (Christchurch and Springston Formations) with loess and swamp deposits in some places. Underlying the Postglacial sediments are predominantly dense Pleistocene age interglacial gravels interbedded with thinner layers of glacial soils. At about 300m depth Pliocene age terrestrial and marginal marine sediments (sand, silt, clay, peat and shell lenses, wood) overlie the basaltic rocks of the Miocene age Banks Peninsula volcanics, which in turn overlie about 400 m of early Tertiary sediments (sandstone, siltstone, conglomerate and coal measures) on Torlesse (greywacke) at about 1200 to 1500 m depth. Most sites in Christchurch CBD are at least Class D, deep soils in terms of NZS 1170.5 site class, and those that experienced liquefaction would have a site class E if the softest soils are more than 10 m thick. Shear wave velocities estimated by correlation with geological/geotechnical description are available for a number of locations and soil shear-wave velocity for surface layers estimated by spatial autocorrelation (SPAC) are available at two locations in Christchurch. One of the locations that have a shear-wave velocity profile down to a depth of 1200m is a GeoNet strong-motion recording station at the Christchurch Botanic Gardens (CBGS) and the other site is the Catholic Cathedral College (CCCC). The shear-wave velocity profiles of the CBGS and CCCC sites are nearly identical and CBGS site is selected for the modelling of site effect in the present study.

Table 4 Shear-wave velocity profile for CBGS site

Depth from	Depth to	Description	V_s (m/sec)
0	19.8	Post Glacial upper	185
19.8	21	Post glacial Lower	300
21	300	Pleistocene	745
300	550	Pliocene	800
550	850	Miocene volcanics	1200
850	1200	Eocene	1000
1200		Greywacke	2000

Four models were used and they have the same shear-wave velocity profile as presented in Table 4 down to a depth of 550m. The first model has a shear-wave velocity profile given in Table 4 down to the depth of 1200m and the shear-wave velocity of the bedrock is 1200m/s. The second model has identical shear-wave velocity profile as given in Table 4 and the bedrock shear-wave velocity of 2000m/s was used. The third model has a depth to 550m and a shear-wave velocity of 1200m/s was used for the bedrock. The fourth model extended the last layer to a depth of 1700m with a bedrock shear-wave velocity of 3000m/s. These models were used to investigate the effect of bedrock depth and shear-wave velocity on the response spectral amplification ratios.

For the soil layers to a depth of 800m, each layer was divided into sub-layers with each sub-layer having a thickness less than 1/5.5 times the shortest wave length (with a maximum frequency of 20Hz) to allow for reasonable accurate modelling of nonlinear soil response. The motions associated with higher frequencies up to 25Hz were used but with less accuracy and the motions associated with frequency higher than 25Hz were removed to improve the converge of iterative nonlinear modelling. Work by Destegul (pers. comm., 2009) has shown that the estimated soil site spectra depend critically on the adopted stress-strain relations. Well-defined profiles of soil shear modulus and density (or shear-wave velocity) are insufficient to constrain the estimated motions. The computer code for the equivalent linear model (SHAKE91) provides ranges of generic stress-strain relations for various types of soils, but there are big differences in the results for the expected ground motions depending on whether the average, upper or lower G/Gmax(γ) relations are adopted (where G is shear modulus and γ is shear strain). These relations are often not well established even by lab tests, because usually tests are carried out only for a limited number of depths and specimen disturbance can have a large effect. Her work has shown also that at large strains SHAKE91 tends to attract strain to a single location (i.e., has a runaway effect in terms of displacement) to a greater extent than a fully nonlinear code like NERA. This leads to an acceleration limiting effect which may or may not be real. These effects occur when G/Gmax falls to less than about 0.5. This artefact does not apply to our study where input ground motions are low. In order to account for uncertainties in soil property characterization, two sets of shear-modulus reduction and shear-strain-dependent damping curves for sand were used for the two top layers and a nonlinear model for soft rock were used for the third and the fourth layers. The thickness of the soil/soft rock layers in Table 4 with a shear-wave velocity over 800m/s was used in the model and linear elastic stress-strain relationship was assumed. The computer code for the equivalent linear model (SHAKE91) makes use of analytical solutions for the wave propagation analyses and accuracy is not related to the layer thickness when an elastic model is used.

Figure 6a presents the NS component amplification ratios for response spectra between the ground surface motion and the synthetic ground motion at a bedrock outcrop site in Christchurch. Model 1 gives a PGA amplification ratio of 1.3 in the NS component and deamplifies the ground motions in a period range of 0.04s-0.2s, as shown in Figure 6a. The largest amplification ratio from model 1 is just over 3 at 0.5s spectral period. For the NS component, the second model increased the amplification by 20% from those from Model 1 at most periods and 30-40% between 0.6 and 2s spectral periods. Model 3 with a depth down to 550m/s on the bedrock with a shear-wave velocity of 1200m/s produced the largest amplification ratios among all models for period up to about 0.7s. The PGA amplification ratio is about 1.8 and the largest amplification ratio is 3.8 at 0.54s. Model 4 has very similar amplification ratios to those of Model 1 for spectral periods up to about 0.7s and has the largest amplification ratio for spectral periods of 2.5-4s.

The amplification ratios for the EW component in Figure 6b are generally very similar to those for the NS component.

Figure 7 shows the response spectra from the synthetic records and the surface ground motions and the amplification ratios from Model 3 which produced the largest amplifications. The synthetic response spectra are amplified at all spectral periods by the soil column and the largest response spectrum is about 0.12g for both horizontal components.

Figure 8 shows the synthetic rock motion and the ground surface motions from Model 3 for the NS component, and Figure 9 shows those of the EW component. The soil site model amplifies the synthetic rock motions by a factor of 1.7 for the NS component and 1.9 for the EW component.

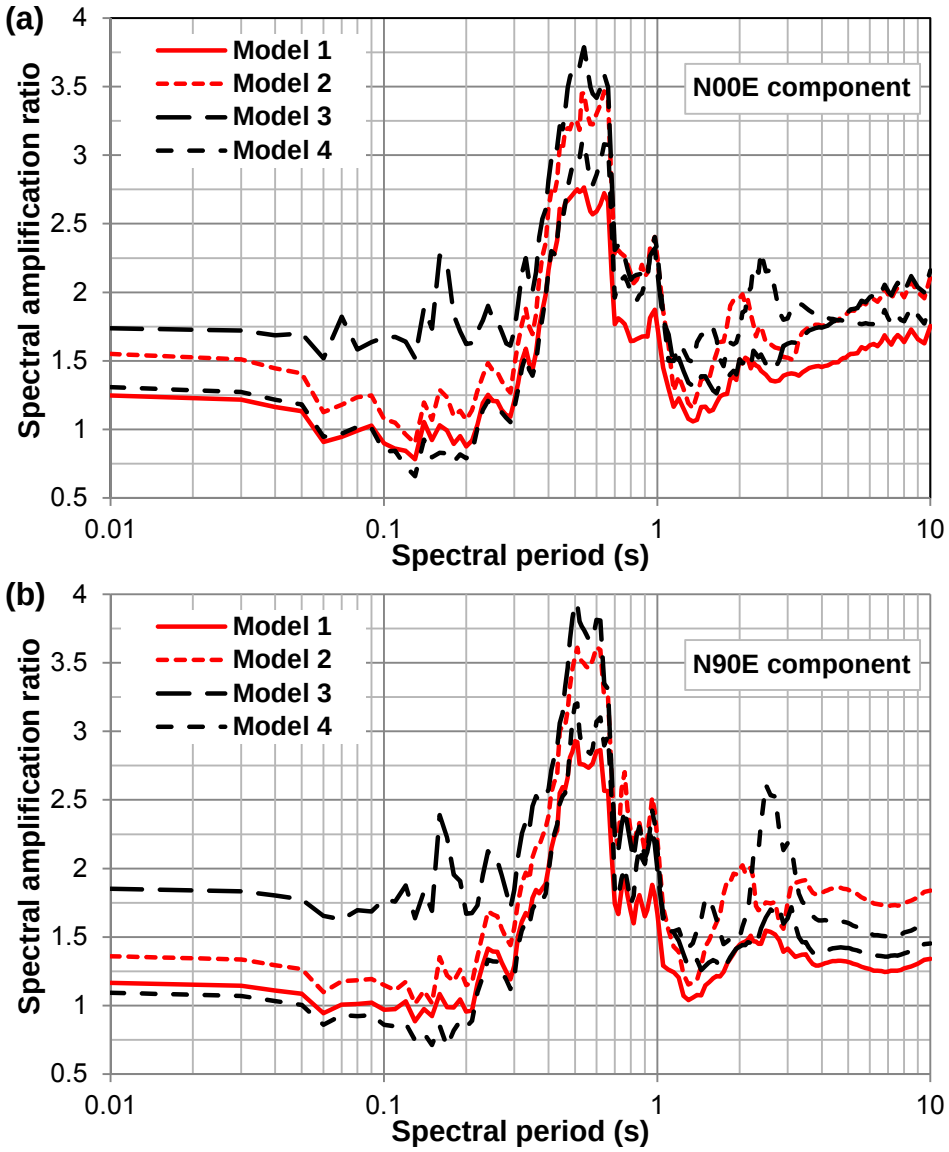

Figure 6 Response spectral amplification ratios for the CBGS site in Christchurch subjected to the synthetic ground motions from a possible Alpine fault event, (a) NS component and (b) EW component.

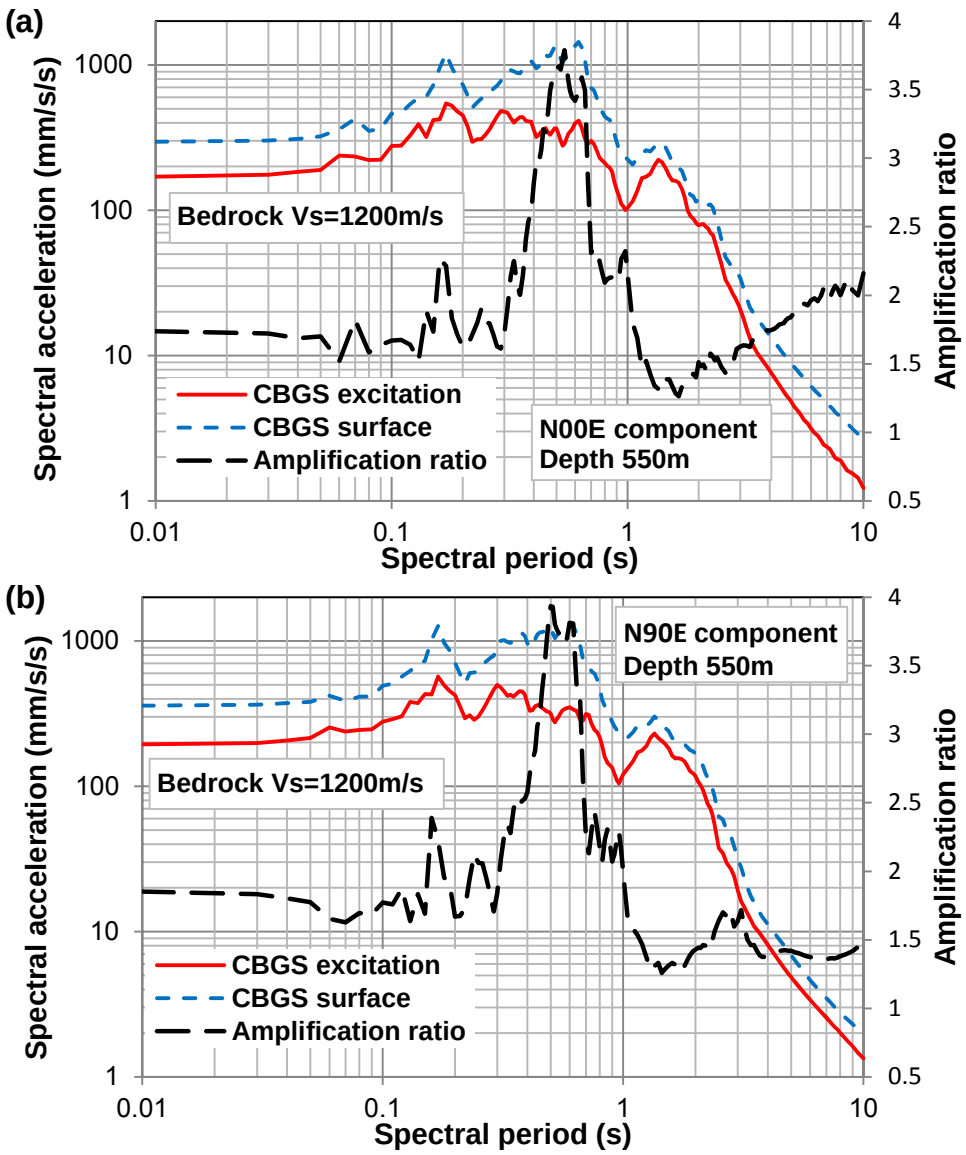

Figure 7 Model 3 response spectra and spectral amplification ratios for the CBGS site in Christchurch subjected to the synthetic ground motions from a possible Alpine fault event, (a) NS component and (b) EW component

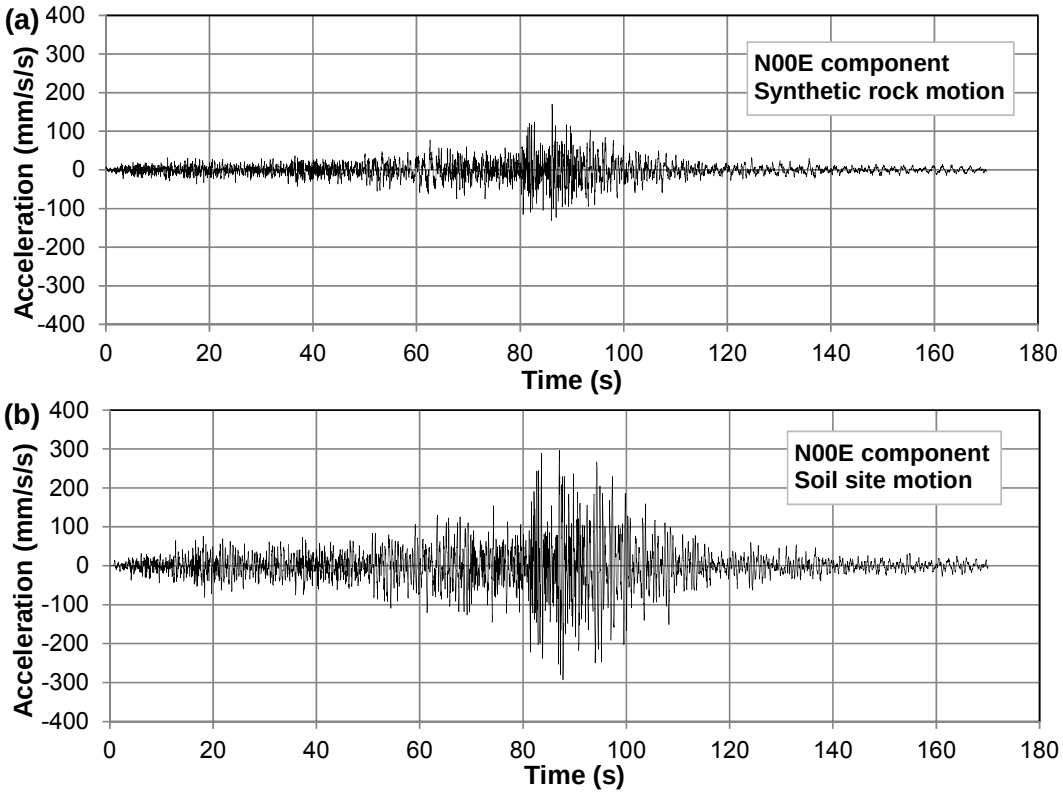

Figure 8 The NS component of the synthetic rock site acceleration time history in (a), and soil surface acceleration time history of Model 3 in (b)

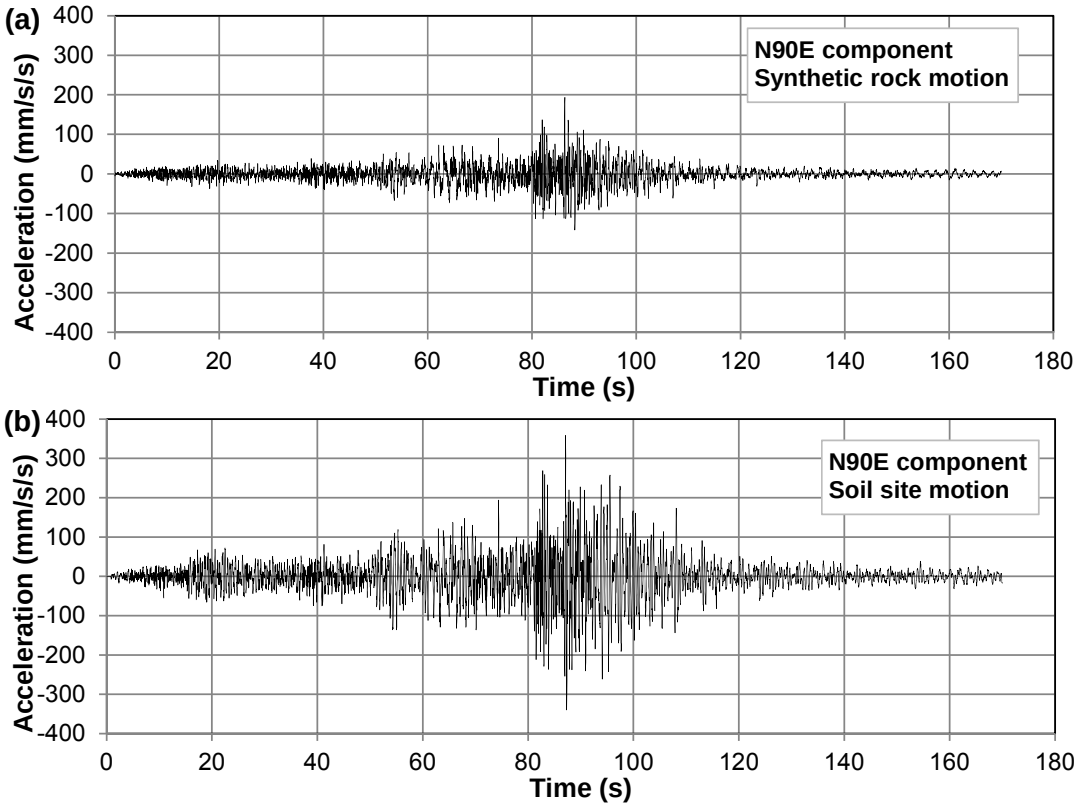

Figure 9 The EW component of the synthetic rock site acceleration time history in (a), and soil surface acceleration time history of Model 3 in (b).

6.0 SUMMARY

Calculations for synthetic seismograms are based on a validated recipe for large crustal earthquakes. Ground motions were calculated using realistic Green's functions, including conservative site effects and for a "worst-case type" rupture scenario for Christchurch city.

Green's functions were selected to be realistically characterizing the source-receiver propagation path and this for each individual asperity. Our Green's function method was limited by the incorrect radiation pattern from the selected Green's functions. However this is unlikely to increase the synthetic accelerations dramatically. Site effects for swampy ground conditions were also added to account for realistic ground conditions in Christchurch. There are uncertainties related to highly variable ground condition in Christchurch, so we took a conservative approach by modelling a range of appropriate geotechnical parameters.

The preliminary computed values of maximum horizontal acceleration are less than 4% g. These results are in agreement with observations for recent large earthquakes (Mw > 7) and distances of 150 km+ (Figure 10).

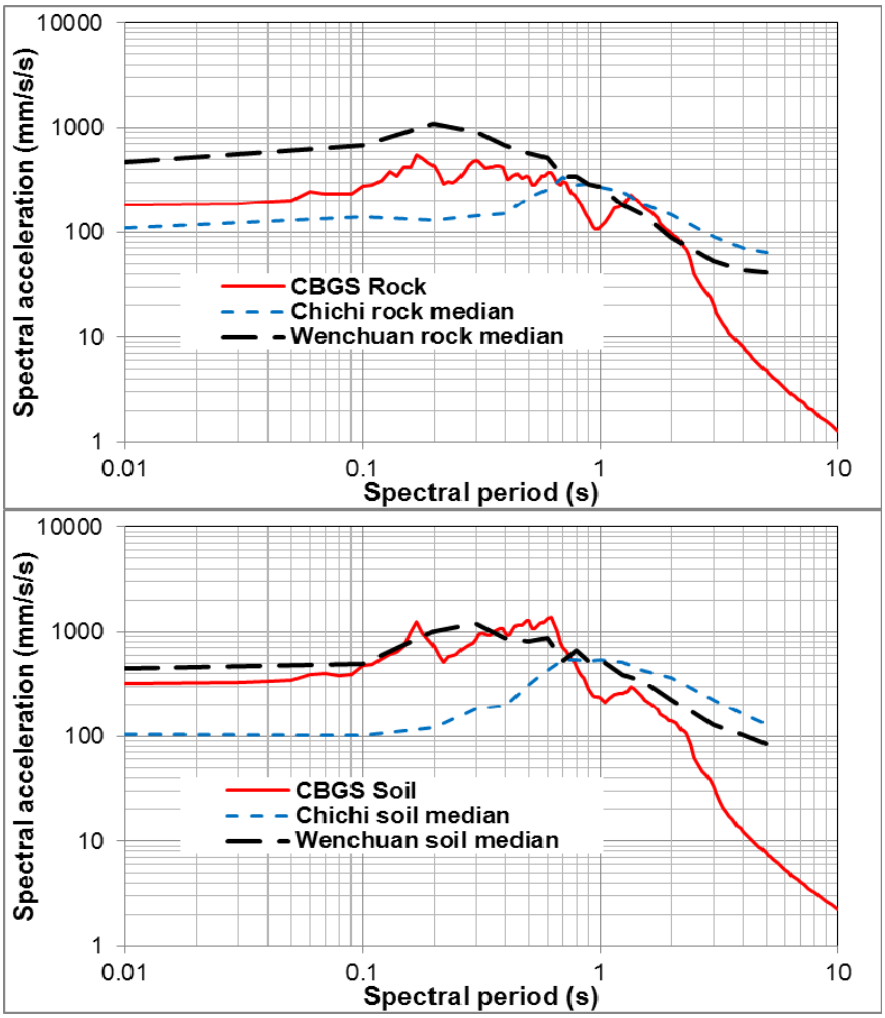

Figure 10 Comparison of response spectra for synthetic ground motion at CBGS on rock (top) and on soil (bottom) with The Mw 7.6 1999 Chichi earthquake and the Mw 7.9 2008 Wenchuan earthquake. The spectra represents the average values at a source distance (closest distance to the fault rupture) of 170 km for two sites with Vs=1200m/s (rock) and 243m/s for soil site.

7.0 REFERENCES

Irikura, K. and Miyake, H. (2011). Recipe for predicting strong ground motion from crustal earthquake scenarios, Pure Appl Geophys, 168, 85–104 doi:10.1007/s00024-010-0150-9.

Irikura, K. : Prediction of strong acceleration motion using empirical Green's function, Proc. 7th Japan Earthq. Eng. Symp., Tokyo, 151-156, 1986.

Kamae, K., K. Irikura, and A. Pitarka: A technique for simulating strong ground motion using hybrid Green's function, Bull. Seism. Soc. Am., 88, 357-367, 1998.

Kurahashi, S., and K. Irikura (2010). Characterized source model for simulating strong ground motions during the 2008 Wenchuan earthquake, Bull. Seismol. Soc. Am. 100, no. 5B, 2450–2475.

Somerville, P., K. Irikura, R. Graves, S. Sawada, D. Wald, N. Abrahamson, Y. Iwasaki, T. Kagawa, N. Smith, and A. Kowada (1999). Characterizing crustal earthquake slip models for the prediction of strong ground motion, Seismol. Res. Lett. 70, no. 1, 59–80.

Sutherland, R.; Eberhart-Phillips, D.; Harris, R.A.; Stern, T.A.; Beavan, R.J.; Ellis, S.M.; Henrys, S.A.; Cox, S.C.; Norris, R.J.; Berryman, K.R.; Townend, J.; Bannister, S.C.; Pettinga, J.; Leitner, B.; Wallace, L.M.; Little, T.A.; Cooper, A.F.; Yetton, M.; Stirling, M.W. 2007 Do great earthquakes occur on the Alpine Fault in central South Island, New Zealand? p. 235-251 IN: Okaya, D.A.; Stern, T.A.; Davey, F.J. (eds) A continental plate boundary: tectonics at South Island, New Zealand. Washington, DC: American Geophysical Union. Geophysical Monograph 175.

Yetton, M. D. 2000. The probability and consequences of the next Alpine fault earthquake, South Island, New Zealand, Ph.D. thesis, Department of Geological Sciences, University of Canterbury, New Zealand.

www.gns.cri.nz

Principal Location

1 Fairway Drive
Avalon
PO Box 30368
Lower Hutt
New Zealand
T +64-4-570 1444
F +64-4-570 4600

Other Locations

Dunedin Research Centre
764 Cumberland Street
Private Bag 1930
Dunedin
New Zealand
T +64-3-477 4050
F +64-3-477 5232

Wairakei Research Centre
114 Karetoto Road
Wairakei
Private Bag 2000, Taupo
New Zealand
T +64-7-374 8211
F +64-7-374 8199

National Isotope Centre
30 Gracefield Road
PO Box 31312
Lower Hutt
New Zealand
T +64-4-570 1444
F +64-4-570 4657